

Angular dependence of the emission wavelength in microcavity organic light emitting diodes

A. B. Djurišić

*Department of Physics and Department of Electrical & Electronic Engineering,
the University of Hong Kong, Pokfulam Road, Hong Kong*

A. D. Rakić and M. L. Majewski

*Department of Information Technology and Electrical Engineering, The University of Queensland,
Brisbane Qld4072, Australia*

In this work, we have calculated the emission wavelength dependence on the viewing angle for different combinations of metallic mirrors. The dispersion of the optical functions of ten different metals is fully taken into account using Lorentz oscillator model. The metals have been assigned to a function of top (cathode) or bottom (anode) mirror based on their work function. Refractive index dispersion of organic layers, N,N'-disphenyl-N,N'-bis(3-methylphenyl)-1,1'-disphenyl-4,4'-diamine (TPD) and tris (8-hydroxyquinoline) aluminum (emitting layer) is taken into account via Cauchy model. The change of the emission wavelength with angle has been calculated iteratively to fully take into account wavelength dependence of indices of refraction and phase change. Calculations have been performed for different hole transport materials and different thickness of the emitting layer.

Keywords: microcavity organic light emitting diodes

1. INTRODUCTION

Organic light emitting diodes are very promising for application in high brightness, large viewing angle flat panel displays. What makes them very attractive is low cost fabrication, possible use of flexible substrates, and ease of fabrication over large area. Lots of progress has been done recently on improving the efficiency and stability of these devices. Further improvements are needed to improve colour purity (emission spectrum of organic compounds is typically very broad), efficiency, and lifetime. Microcavity organic light emitting diodes have been used in order to improve extraction efficiency and colour purity of organic light emitting diodes.¹⁻¹¹ However, due to broad emission from organic material, organic microcavity devices exhibit one undesirable property, blue shift of the emission wavelength with the increasing viewing angle. Experimentally determined emission wavelength shift in tris (8-hydroxyquinoline) aluminum (Alq₃) is quite large. Emission wavelength shifts with viewing angle in Alq₃ based MOLEDs as large as from 580 nm to ~530 nm at 50°, from 560nm to ~530 nm at 40°,⁶ from 610 nm to ~500 nm at 80°, and from 540nm to ~500 nm at 50°⁷ were reported. In spite of the significance of this phenomenon, theoretical studies of this phenomenon have been scarce.^{10,11}

The physical basis of the emission wavelength shift with the viewing angle was addressed only for silver/poly(p-phenylene vinylene) (PPV)/silver microcavities using a simple model.^{10,11} Becker *et al.*¹⁰ investigated the position of the resonance wavelength for different silver mirror thickness. They concluded that angular dependence would be minimized using thicker metal films. Tessler *et al.*¹¹ have used a simple equation

$$\lambda = 2\pi m L_{eff} n \cos(\theta) \quad , \quad (1)$$

where m is the mode number, n is the material inside the cavity, θ is internal angle, and L_{eff} is the effective cavity length which includes any additional length introduced by the mirrors. Based on the equation above, they conclude that in order to decrease wavelength shift as $\cos(\theta)$ decreases, L_{eff} and/or n should increase. This simplified analysis, however, does not

provide any detailed insight into the wavelength dependence on the viewing angle, nor takes into account the wavelength and angle dependence of the phase shift upon reflection from the mirrors.

In this work, we provide detailed analysis of the emission wavelength dependence on the viewing angle in Alq₃ based MOLEDs. We derived a model for the resonant wavelength shift and used an iterative procedure to calculate this shift which fully takes into account the dispersion in the organic layers, wavelength dependence of the index of refraction in the metal mirrors, and the wavelength and angle dependence of the phase shift upon reflection from the metal mirrors. We have chosen MOLEDs with both metal mirrors since metal mirrors allow higher brightness enhancement.¹² Different metals were considered for top or bottom mirrors based on their work function (high work function metals for the bottom mirror/anode, low work function metals for the top mirror/cathode). The paper is organized as follows. In the following section, the model is described. In section 3, obtained results are presented and discussed. Finally, conclusions are drawn.

2. DESCRIPTION OF THE MODEL

The resonant modes of a microcavity have to satisfy the condition that the phase change during one round trip is a multiple of 2π . In other words, for normal incidence, the following equation is valid:

$$\sum_i \frac{4\pi d_i n_i(\lambda)}{\lambda} - \varphi_{top}(0, \lambda) - \varphi_{bot}(0, \lambda) = 2m\pi \quad , \quad (1)$$

where λ is the emission wavelength, $\varphi_{top}(0, \lambda)$, $\varphi_{bot}(0, \lambda)$ are the angle and wavelength dependent phase change upon reflection from top and bottom mirrors, respectively, m is an integer which defines the mode number, and the summation in is performed over all the layers inside the cavity with thicknesses d_i and refractive indices $n_i(\lambda)$. For oblique incidence, the resonant wavelengths are solutions of the following equation:

$$\sum_i \frac{4\pi d_i n_i(\lambda + \Delta\lambda) \cos \theta_i}{\lambda + \Delta\lambda} - \varphi_{top}(\theta_{top}, \lambda + \Delta\lambda) - \varphi_{bot}(\theta_{bot}, \lambda + \Delta\lambda) = 2m\pi \quad , \quad (2)$$

where θ_{top} , θ_{bot} are incidence angles at top and bottom mirrors, respectively, while θ_i is the angle of propagation within i -th organic layer. From Eqs.(1) and (2), the following expression for the wavelength shift $\Delta\lambda$ can be obtained:

$$\Delta\lambda = \frac{1}{\Delta\Phi} \left\{ \sum_i 4\pi d_i [n_i(\lambda + \Delta\lambda) \cos \theta_i - n_i(\lambda)] - \lambda(\Delta\varphi_{top} + \Delta\varphi_{bot}) \right\} \quad , \quad (3)$$

where

$$\Delta\Phi = 2m\pi + \varphi_{top}(\theta_{top}, \lambda + \Delta\lambda) + \varphi_{bot}(\theta_{bot}, \lambda + \Delta\lambda) \quad , \quad (4)$$

$$\Delta\varphi_{top} = \varphi_{top}(\theta_{top}, \lambda + \Delta\lambda) - \varphi_{top}(0, \lambda) \quad , \quad (5)$$

$$\Delta\varphi_{bot} = \varphi_{bot}(\theta_{bot}, \lambda + \Delta\lambda) - \varphi_{bot}(0, \lambda) \quad . \quad (6)$$

Since Eq.(3) contains several terms which are wavelength dependent, iterative procedure was used to calculate the wavelength shift $\Delta\lambda$. The starting point was the wavelength shift calculated for the case of no dispersion, and the procedure was terminated when the change in $\Delta\lambda$ in two consecutive iterations was smaller than 0.1 nm. As can be observed from Eq. (3), the wavelength shift with viewing angle is inversely proportional to the mode number m . However, no significant improvement can be obtained by increasing m , since this also requires larger thickness of the organic layers d_i , and $\Delta\lambda$ is

directly proportional to the thickness values of organic layers. Therefore, the cavity order has no significant influence on the emission wavelength shift (typically less than 1 nm difference for neighboring modes ($m=1,2$; $m=2,3$ etc.)). However, maximum achievable extraction efficiency η_{max} is inversely proportional to the mode number m . Therefore, low order ($m=1,2$) cavities are preferred for attaining high extraction efficiency. In order to achieve maximum efficiency, emitting layer should be located at the maximum field in the cavity. For $m=1$, field maximum is at the mirrors, and placing the emission layer close to organic/metal interface could cause significant exciton quenching. Therefore, in our calculations we will consider cavities with $m=2$.

The microcavity structure considered here is glass substrate/bottom mirror/HTL/ETL/top mirror, where HTL denotes hole transport layer and ETL denotes electron transport layer. Alq₃ was considered for ETL, while for HTL N,N'-disphenyl-N,N'-bis(3-methylphenyl)-1,1'-disphenyl-4,4'-diamine (TPD) or copper phthalocyanine (CuPc) were considered. The phase shift upon reflection from the metal mirror was obtained by calculating the reflectance at metal/organic interface. The phase shift upon reflection is fully determined with the complex index of refraction $N_m(\lambda)=n_m(\lambda)-ik_m(\lambda)$, refractive index of organic material $n_i(\lambda)$ (hole transport layer for the bottom mirror, Alq₃ for the top mirror), the angle in the metal θ_m , and the angle within organic layer θ_i . In case of the bottom mirror, the glass substrate needs to be considered as well. The angles in the equations describing the resonant wavelength shift are related to the viewing angle outside cavity θ_0 via Snell's law $N_m \sin \theta_m = n_i \sin \theta_i = \sin \theta_0$. The wavelength dependence of the index of refraction for the metals was modeled using oscillator model, with model parameters given in Ref.¹³ The refractive index of Alq₃ and TPD was modeled using Cauchy equation $n(\lambda)=A+B/\lambda^2+C/\lambda^4$, where the coefficients A , B , and C were determined by fitting the data in Ref.¹⁴ CuPc has low absorption in the spectral region 450-550 nm.¹⁵ However, the experimental data for CuPc in that spectral range¹⁵ cannot be well described with Cauchy equation, so that a polynomial fit was used. Metals with work function ϕ higher than 4.5 eV have been considered for bottom mirror since bottom mirror also serves as anode and should provide efficient hole injection. Therefore, Al, Ag, Cr, and Ti ($\phi=4.28$ eV, 4.26 eV, 4.5 eV, and 4.3 eV, respectively¹⁶) were assigned for top mirror, while Au, Pt, Ni, and Cu ($\phi=5.1$ eV, 5.65 eV, 5.15 eV, and 4.65 eV, respectively¹⁶) were used for bottom mirror. Due to superior optical quality of silver thin films and lowest absorption in the visible region of all metals considered, we have also considered MOLEDs with both silver mirrors.

For the bottom mirror, phase change upon reflection was determined by applying matrix formalism with incoherent substrate correction to calculate reflectance from the thin metal film on a glass substrate. The refractive index of glass was described with Cauchy equation. The light was incident from HTL. The thickness of the semitransparent bottom metal mirror was determined from the condition for the reflectivity of the mirror to achieve optimal extraction of light from a microcavity LED:¹⁷

$$R_1 = \min(R_1^{crit}, R_1^{sp,crit}, R_1^{loss}) \quad , \quad (9)$$

where

$$R_1^{crit} = 1 - \frac{m}{n^2} \quad , \quad (10)$$

where m is the mode number, and n is the refractive index of the material inside the cavity, R_1^{loss} is determined by the losses in the cavity (for large losses, approximately equal to the reflectivity of the top mirror R_2), and

$$R_1^{sp,crit} = 1 - 2mS \quad , \quad (11)$$

where S is the relative spectral width $S = \Delta k/k_0$ obtained by dividing FWHM of the emission spectra of the material with the central frequency. Due to broad emission inherent to majority of the organic materials, the reflectance of the bottom mirror is limited by $R_1^{sp,crit}$. Spectral width for the Alq₃ emission is $S \approx 0.16$, so that for $m=1$ the reflectance of the bottom mirror

should be $R_1 \approx 0.68$, and for $m=2$, it should be $R_1 \approx 0.36$. Based on this value, we have determined the required thickness for the bottom mirror.

3. RESULTS AND DISCUSSION

Figure 1 shows the phase change as a function of viewing angle for the top and bottom mirror. Due to the difference in phase change dependence for the s and p polarizations, the resonant wavelength shift will be different. The calculated resonant wavelength shifts for the different cavity lengths and hence different resonant wavelengths for $\theta_0=0^\circ$ are shown in Fig. 2. It can be observed that the resonant wavelength shift becomes smaller for shorter wavelengths. The shift for $\lambda=480$ nm is about twice smaller than the shift for $\lambda=600$ nm. This is a consequence of higher dispersion in the organic layers and therefore lower value of the term $(n_i(\lambda + \Delta\lambda)\cos\theta_i - n_i(\lambda))$ resulting in smaller resonant wavelength shift. Therefore, in designing MOLEDs operating wavelength on the short wavelength side of the emission peak of the light emitting material should be chosen. This will ensure that the resonant wavelength shift would be as low as possible for a given device structure.

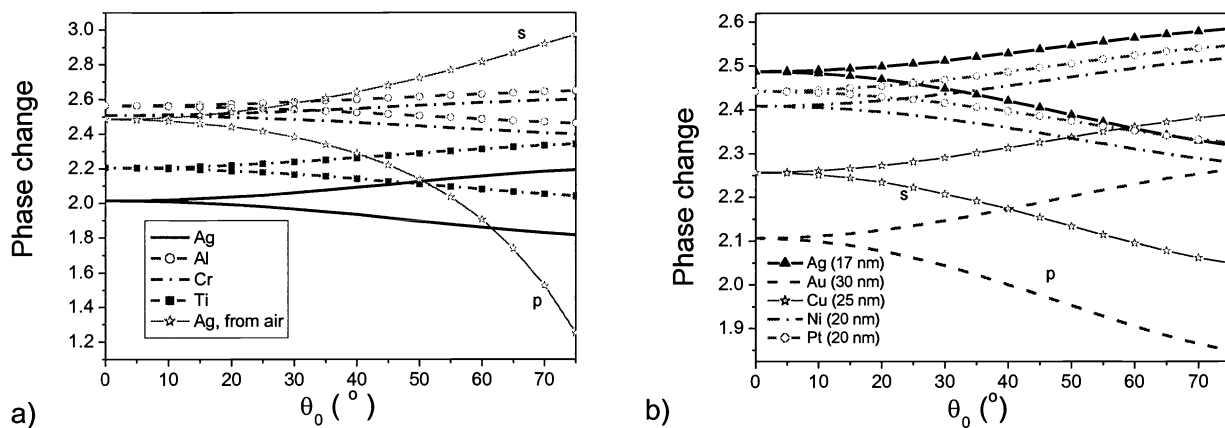


Fig. 1 a) The phase change upon reflection from the top mirror. Light is incident from Alq₃. b) The phase change for Ag-air interface is also shown. b) The phase change upon reflection from the bottom mirror. The light is incident from TPD.

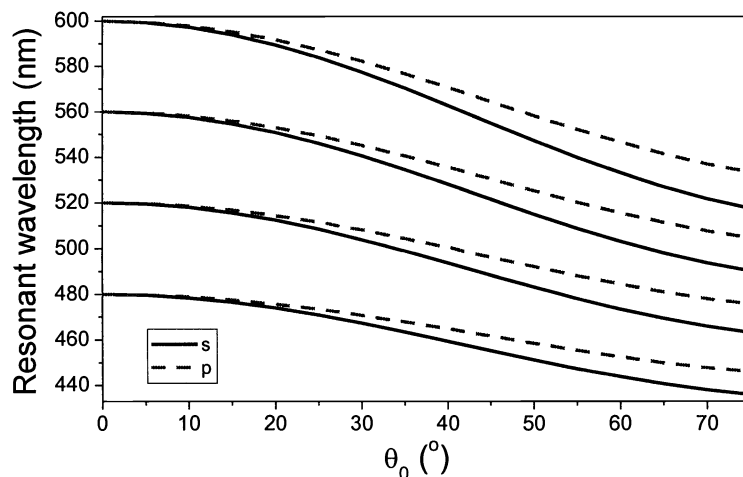


Fig. 2 The resonant wavelengths shift for different effective cavity lengths

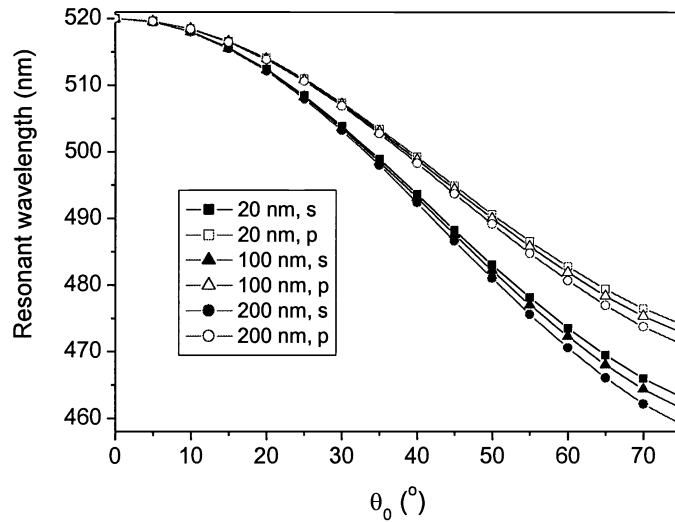


Fig. 3 The resonant wavelength shift for different thickness of Alq₃ layer.

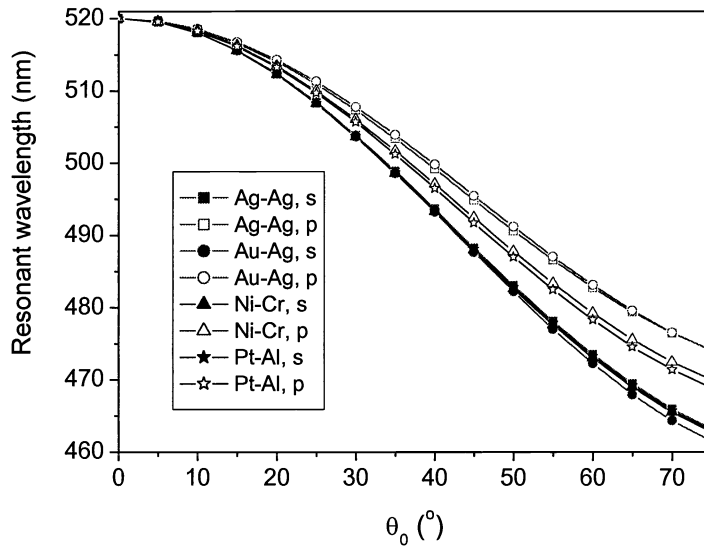


Fig. 4 The resonant wavelength shift for different choice of the top and bottom mirrors.

Since Alq₃ and TPD have similar value of the refractive index at $\lambda=520$ nm but TPD is more dispersive, we investigated the influence of the Alq₃ thickness on the resonant wavelength shift. Obtained results are shown in Fig. 3. It can be observed that the resonant wavelength shift is smaller for thinner Alq₃ layers. Therefore, we adopted Alq₃ thickness of 20 nm for other calculations. We also investigated influence of the choice of the metal mirrors. The resonant wavelength shift was calculated for different high work function metal (bottom) and low work function metal (top) mirror combinations (Ag-

Ag, Ag-Au, Ag-Ni, Ag-Pt, Ag-Cu; Al-Ag, Al-Au, Al-Ni, Al-Pt, Al-Cu, Ti-Ag, Ti-Au, Ti-Ni, Ti-Pt, Ti-Cu, Cr-Ag, Cr-Au, Cr-Ni, Cr-Pt, and Cr-Cu). Selected results (two of the best and two of the worst results) are shown in Fig. 4. It can be observed that the changes for s polarization are small, while mirror choice has more effect on the resonant wavelength shift for the p polarization. However, the degree of the improvement which can be achieved via choosing the mirrors which yield the lowest resonant wavelength shift is very limited. The major part of the resonant wavelength shift is due to the change of the optical path inside the cavity with the change of the viewing angle. To minimize this change, more dispersive materials are needed.

Majority of organic materials have low dispersion and low refractive index in the spectral region below the first absorption band. In order to explore the possibility of reduction of the resonant wavelength shift with the viewing angle, we have performed calculations for a hypothetical composite material. Composite organic/inorganic materials are promising for the improvement of electrical and optical properties of organic materials, while the advantages of easy and inexpensive manufacture are retained. It has been demonstrated that high refractive index and increased dispersion can be achieved in hybrid polymer-inorganic films.¹⁸ Synthesis of small nanoparticles of variety of materials,^{19,20} including GaP nanoparticles with 9 nm average size,²¹ has been reported. Therefore, preparation of composite polymer/inorganic semiconductor films is feasible and it may be useful option to explore in order to achieve greater variation in refractive index parameters of layers in organic devices. We have chosen to simulate a composite consisting of GaP nanoparticles in bisphenyl-A polycarbonate (PC). GaP has been chosen as a semiconductor with high refractive index and suitable bandgap value (transparent in green spectral region). The refractive index of PC²² and GaP²³ were taken from the literature, and the dielectric function $\langle \epsilon \rangle$ and hence the index of refraction of the composite film was calculated using effective medium approximation:²⁴

$$\frac{\epsilon_a - \langle \epsilon \rangle}{\epsilon_a + 2\langle \epsilon \rangle} f_a + \frac{\epsilon_b - \langle \epsilon \rangle}{\epsilon_b + 2\langle \epsilon \rangle} (1 - f_a) = 0 \quad (13)$$

where ϵ_a and ϵ_b are the dielectric function values of two components, f_a is the volume fraction of the component a .

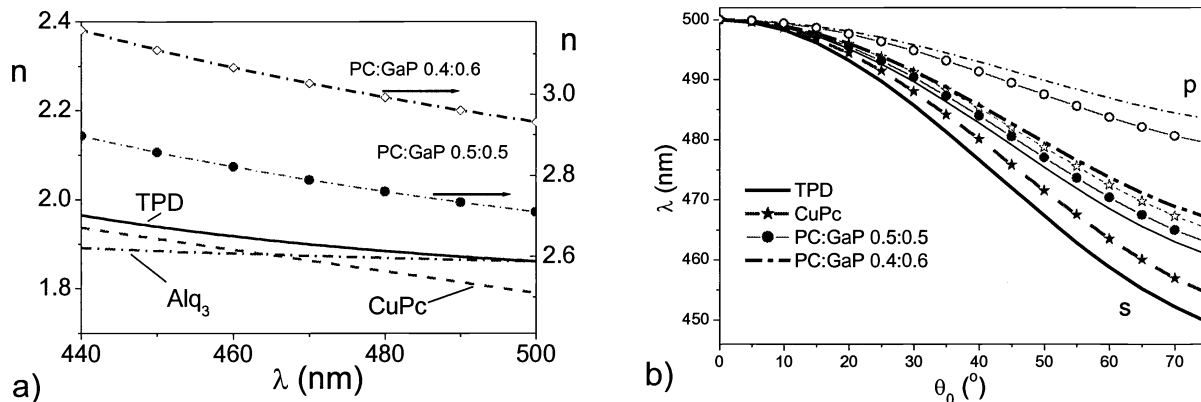


Fig. 5 The dispersion in different hole transport layers. Wavelength dependence of the refractive index of Alq_3 is also shown. b) The resonant wavelength shift for different hole transport layers.

The refractive index dependence on the wavelength for different materials and the resonant wavelength shift for MOLEDs with different hole transport layers is shown in Fig. 5. It can be observed that the resonant wavelength shift is smaller for CuPc compared to TPD. More significant reduction in the resonant wavelength shift could be achieved with composite organic/inorganic materials. However, optimization of the choice of materials and the mirrors is not sufficient to

eliminate this phenomenon. Therefore, more narrow organic emitters should be considered for MOLED applications. If the emission spectrum is narrow, viewing angle will be smaller, but significant colour change with the viewing angle increase will be avoided. Also, narrow emission spectrum of the emitting material would place less stringent limit on the reflectance of the bottom mirror to achieve brightness enhancement. Another option worth considering is the use of Bragg mirrors with phase shift adjusted to compensate for the change of the optical path in the organic material.

4. CONCLUSION

In conclusion, we have developed a model for the emission wavelength dependence on the viewing angle in organic microcavity light emitting diodes with metal mirrors. We have found that the main contribution to the wavelength shift originates in the change of the optical path inside the organic materials. Therefore, the wavelength shift can be reduced by using more dispersive materials. The resonant wavelength shift for the p polarization is more sensitive to the mirror choice, and Ag-Au and Ag-Ag configurations represent the most suitable choices. Even with the optimal choice of mirrors and the materials within the cavity, it is not possible to eliminate this effect in MOLEDs with two metal mirrors. Different Bragg mirror designs should be investigated for possible reduction of the resonant wavelength shift in MOLEDs. Also, use of emitting material with more narrow emission spectrum is advisable.

ACKNOWLEDGEMENTS

This work the University of Hong Kong University Research Committee seed funding grant.

REFERENCES

1. B. Zhang, Y. Ma, M. Xu, K. Wu, C. Huang, Y. Zhao, D. Zhuo, L. Yin, and X. Zhao, "Planar organic microcavity of Eu-chelate film with metal mirrors", *Solid State Commun.* **104**, pp. 593-596, Dec 1997.
2. A. Dodabalapur, L. J. Rothberg, and T. M. Miller, "Color variation with electroluminescent organic semiconductors in multimode resonant cavities" *Appl. Phys. Lett.* **65**, pp. 2308-2310, Oct. 1994.
3. S. Tokito, K. Noda, and Y. Taga, "Strongly directed single mode emission from organic electroluminescent diode with a microcavity", *Appl. Phys. Lett.* **68**, 2633-2635, May 1996.
4. X. Y. Liu, L. X. Wang, Y. Liu, S. L. E, J. M. Zhao, D. J. Wu, Y. Q. Ning, S. L. Wu, L. J. Wang, C. J. Liang, D. X. Zhao, Z. R. Hong, D. Zhao, C. Q. Jin, X. B. Jing, F. S. Wang, W. L. Li, and S. T. Lee, "Spontaneous emission properties of organic film in plane optical microcavity", *Thin Solid Films* **363**, pp. 204-207, March 2000.
5. J. Grüner, F. Cacialli, and R. H. Friend, "Emission enhancement in single-layer conjugated polymer microcavities", *J. Appl. Phys.* **80**, pp. 207-215, July 1996.
6. R. H. Jordan, L. J. Rothberg, A. Dodabalapur, and R. E. Slusher, "Efficiency enhancement of microcavity organic light emitting diodes", *Appl. Phys. Lett.* **69**, pp. 1997-1999, Sept. 1996.
7. S. Dirr, S. Wiese, H.-H. Johannis, D. Ammermann, A. Böhrer, W. Grahn, and W. Kowalsky, "Luminescence enhancement in microcavity organic multilayer structures", *Synthetic Metals* **91**, pp. 53-56, Dec. 1997.
8. A. Dodabalapur, L. J. Rothberg, R. H. Jordan, T. M. Miller, R. E. Slusher, and J. M. Phillips, "Physics and applications of organic microcavity light emitting diodes", *J. Appl. Phys.* **80**, pp. 6954-6964, Dec. 1996.
9. N. Takada, T. Tsutsui, and S. Saito, "Control of emission characteristics in organic thin film electroluminescent diodes using an optical microcavity structure", *Appl. Phys. Lett.* **63**, pp. 2032-2034, Oct. 1993.
10. H. Becker, S. E. Burns, N. Tessler, and R. H. Friend, "Role of optical properties of metallic mirrors in microcavity structures", *J. Appl. Phys.* **81**, pp. 2825-2829, March 1997.
11. N. Tessler, S. Burns, H. Becker, and R. H. Friend, "Suppressed angular color dispersion in planar microcavities", *Appl. Phys. Lett.* **70**, pp. 556-558, Feb. 1997.
12. K. Neyts, P. De Visschere, D. K. Fork, and G. B. Anderson, "Semitransparent metal or distributed Bragg reflector for wide-viewing-angle organic light-emitting-diode microcavities", *J. Opt. Soc. Am. B* **17**, pp. 114-119, Jan. 2000.

13. A. D. Rakić, A. B. Djurišić, J.M. Elazar and M. L. Majewski, "Optical properties of metallic films for vertical-cavity optoelectronic devices", *Appl. Opt.* **37**, pp. 5271-5283, Aug. 1998.
14. F. G. Celii, T. B. Harton, and D. F. Philips, "Characterization of organic thin films for OLEDs using spectroscopic ellipsometry", *J. Electron. Mater.* **26**, pp. 366-371, April 1997.
15. A. B. Djurišić, C. Y. Kwong, T. W. Lau, W. L. Guo, E. H. Li, Z. T. Liu, H. S. Kwok, L. S. M. Lam, and W. K. Chan, *Opt. Commun.* **205**, pp. 155-162, April 2002.
16. H. B. Michaelson, "The work function of the elements and its periodicity", *Journal of Applied physics* **48**, pp. 4729-4733, Nov. 1977.
17. H. Benisty, H. De Neve, and C. Weisbuch, "Impact of planar microcavity effects on light extraction-Part I: basic concepts and analytical trends". *IEEE Journal of Quantum Electronics* **34**, pp. 1612-1631, Sept. 1998.
18. C.-C. Chang and W.-C. Chen, "High-refractive-index thin films prepared from aminoalkoxysilane-capped pyromellitic dianhydride-titania hybrid materials", *Journal of Polymer Science Part A: Polymer Chemistry* **39**, pp. 3419-3427, Oct. 2001.
19. M. Benaissa, K. E. Gonslaves, and S. P. Rangarajan. "AlGaIn nanoparticle/polymer composite: synthesis, optical, and structural characterization", *Appl. Phys. Lett.* **71**, pp. 3685-3697, Dec. 1997.
20. C. Lam, Y. F. Zhang, Y. H. Tang, C. S. Lee, I. Bello, and S. T. Lee, "Large-scale synthesis of ultrafine Si nanoparticles by ball milling", *J. Crystal Growth* **220**, pp. 466-470, Dec. 2000.
21. S. Gao, D. Cui, B. Huang, and M. Jiang, "Study on the factors affecting the particles size of GaP nanocrystalline materials", *J. Crystal Growth* **192**, pp. 89-92, Aug. 1998.
22. H. R. Philipp, D. G. Legrand, H. S. Cole, and Y. S. Liu, "The optical properties of bisphenol-A polycarbonate", *Polymer Engineering and Science* **27**, pp. 1148-55, Aug. 1987.
23. A. Borghesi and G. Guizzetti, in E. D. Palik Ed., *Handbook of Optical Constants of Solids I*, Academic Press Inc., Orlando, Fl., (1985) pp. 445.
24. D. E. Aspnes, J. B. Theeten, and F. Hottier, "Investigation of effective-medium models of microscopic surface roughness by spectroscopic ellipsometry", *Phys. Rev. B* **20**, pp. 3292-3302, Oct. 1979.